Molecular Biology of the Cell
Vol. 13, 211–224, January 2002

Fission Yeast F-box Protein Pof3 Is Required for Genome Integrity and Telomere Function

Satoshi Katayama,* Kenji Kitamura,*† Anna Lehmann,* Osamu Nikaido,‡ and Takashi Toda*§

*Laboratory of Cell Regulation, Imperial Cancer Research Fund, London WC2A 3PX, United Kingdom; and ‡Laboratory of Molecular and Cellular Pharmacology, Department of Pharmacology, Kanazawa University, Ishikawa 920-1192, Japan

Submitted July 5, 2001; Revised October 4, 2001; Accepted October 5, 2001
Monitoring Editor: Howard Riezman

The Skp1-Cullin-1/Cdc53-F-box protein (SCF) ubiquitin ligase plays an important role in various biological processes. In this enzyme complex, a variety of F-box proteins act as receptors that recruit substrates. We have identified a fission yeast gene encoding a novel F-box protein Pof3, which contains, in addition to the F-box, a tetratricopeptide repeat motif in its N terminus and a leucine-rich-repeat motif in the C terminus, two ubiquitous protein–protein interaction domains. Pof3 forms a complex with Skp1 and Pcu1 (fission yeast cullin-1), suggesting that Pof3 functions as an adaptor for specific substrates. In the absence of Pof3, cells exhibit a number of phenotypes reminiscent of genome integrity defects. These include G2 cell cycle delay, hypersensitivity to UV, appearance of lagging chromosomes, and a high rate of chromosome loss. *pof3* deletion strains are viable because the DNA damage checkpoint is continuously activated in the mutant, and this leads to G2 cell cycle delay, thereby preventing the mutant from committing lethal mitosis. Pof3 localizes to the nucleus during the cell cycle. Molecular analysis reveals that in this mutant the telomere is substantially shortened and furthermore transcriptional silencing at the telomere is alleviated. The results highlight a role of the SCF^{Pof3} ubiquitin ligase in genome integrity via maintaining chromatin structures.

INTRODUCTION

The ubiquitin-proteasome–dependent proteolysis plays a pivotal role in a variety of systems (Hershko and Ciechanover, 1992; Hochstrasser, 1996). This proteolytic pathway consists of a series of enzymatic reactions involving a ubiquitin-activating enzyme (E1), a ubiquitin-conjugating enzyme (E2), and finally a ubiquitin ligase (E3). The E3 ubiquitin ligase is required for determining the timing and specificity of protein degradation. There are a number of E3 species in a single organism such as the HECT domain and RING finger proteins (Freemont, 2000).

A multiprotein complex, the SCF ubiquitin ligase, consists of at least four subunits, Skp1, Cullin-1, the RING finger Rbx1/Roc1/Hrt1 and F-box proteins (SCF stands for underlined components) (Peters, 1998; Zachariae and Nasmyth, 1999; Jackson *et al.*, 2000; Tyers and Jorgensen, 2000). Although the first three subunits are common core components of the SCF, F-box proteins comprise multiple different molecules. The F-box consists of 50 amino acid residues and represents a motif required for Skp1 binding (Bai *et al.*, 1996). It is the F-box protein that plays a major role in substrate recognition in the SCF, and accordingly it is called a substrate-specific receptor (Feldman *et al.*, 1997; Skowyra *et al.*, 1997). In budding yeast 16 F-box proteins are encoded in the genome (Bai *et al.*, 1996; Patton *et al.*, 1998), whereas in metazoans the number exceeds at least 30 (Cenciarelli *et al.*, 1999; Regan-Reiman *et al.*, 1999; Winston *et al.*, 1999). Thus, to understand a cellular role of the SCF ubiquitin ligase as a whole, systematic characterization of individual F-box proteins would be one of the most orthodox routes. In this context, budding yeast and fission yeast are ideal model organisms by which to explore this question, because the entire genome has been sequenced, and both forward and reverse genetics is more amenable compared with other experimental systems.

For successive cell divisions, accurate chromosome segregation is a key event. To achieve an equal partitioning of genetic information, both *cis*-acting sequence and *trans*-act-

DOI: 10.1091/mbc.01–07-0333.
† Present address: Center for Gene Science, Hiroshima University, Kagamiyama 1-4-2, Higashi-Hiroshima 739-8527 Japan.
§ Corresponding author. E-mail address: toda@icrf.lif.uk.
Abbreviations used: GFP, green fluorescence protein; HU, hydroxyurea; PCR, polymerase chain reaction; ts, temperature sensitive.

ing factors play an interdependent role. *cis* elements include centromeres and telomeres on chromosomes, whereas *trans* factors comprise structural and regulatory molecules involved in kinetochore and telomere function. The cell is constantly exposed to an antagonistic environment, such as DNA-damaging agent, deprivation of the nucleotide pool, and spindle destruction. To circumvent these harmful conditions, the cell has developed surveillance mechanisms, collectively called checkpoint (Hartwell and Weinert, 1989; Murray, 1995). Failure in checkpoint activation under adverse conditions will lead to uncontrolled cell cycle progression without arrest and repair, resulting in genome ploidy defects (Hartwell *et al.*, 1994; Lengauer *et al.*, 1998). In particular, cancerous cells are often associated with aneuploidy and understanding the underlying mechanisms of accurate chromosome segregation is one of the goals for basic biology (Nasmyth *et al.*, 2000; Hoeijmakers, 2001).

Recent molecular analysis of the telomere has established an essential role for this specialized structure not only in the protection of the end of linear chromosomes and its replication but also in genome integrity in general (Lingner and Cech, 1998; Cooper, 2000). Telomere length, albeit varied from species to species and cell to cell, is tightly regulated with regard to proliferation capacity and cellular senescence. Furthermore, the telomere-proximal regions contain heterochromatin, which displays a specific higher order chromatin structure causing gene expression to be repressed (known as silencing).

Previously, we isolated five independent alleles of temperature-sensitive (ts) *skp1* mutants. Phenotypic analysis of these mutants showed that, despite some variations in defective phenotypes, all the mutants showed G2 cell cycle delay (Yamano *et al.*, 2000; Lehmann and Toda, unpublished data). In contrast, mutations in two previously characterized F-box proteins, Pop1 and Pop2, result in polyploid phenotypes, which are attributable to the accumulation of Cdc18 (an S-phase regulator) and Rum1 (an inhibitor of Cdc2) (Kominami and Toda, 1997; Kominami *et al.*, 1998). We, therefore, reasoned that another F-box protein must exist, which is responsible for this G2 cell cycle delay in ts *skp1* strains. In this study we have identified a novel F-box protein Pof3 in fission yeast, the mutation of which displays G2 cell cycle delay. We show that Pof3 plays a crucial role in overall genome integrity and is required for the maintenance of telomere length and transcriptional silencing at the telomere.

MATERIALS AND METHODS

Strains, Media, Genetic Methods, and Nomenclatures

Strains used in this study are listed in Table 1. YPD (2% dextrose, 2% polypeptone, and 1% yeast extract) and YE5S were used as rich media and modified synthetic EMM2 was used as minimal medium. For minichromosome loss assay, rich YE medium lacking additional auxotrophic supplements was used. Standard methods were followed as described (Moreno *et al.*, 1991). Gene disruptions are abbreviated as the gene proceeded by Δ such as Δ*pof3*. Proteins are designated by an uppercase first letter, e.g., Pof3.

Identification of Schizosaccharomyce pombe *Open Reading frames (ORFs) That Encode F-box Proteins*

An *S. pombe* genomic database (Sanger Center, Hixton, United Kingdom) was searched with the F-box sequence taken from Pop1 and Pop2 as a query. In parallel, a homology search with 16 budding yeast F-box proteins as queries was also performed. F-box regions of each candidate were then visually inspected after alignment with the F-box consensus sequence. In this way, in addition to Pop1 and Pop2, 13 novel F-box proteins have been identified from the fission yeast genome (Pof1-Pof13; this study; Katayama, Harrison, and Toda, unpublished data).

Nucleic Acids Preparation and Manipulation

Enzymes were used as recommended by the suppliers (New England Biolabs, Beverly, MA). Nucleotide sequence data reported in this article are in the DDBJ/EMBL/GenBank databases under accession number AB032411 (*pof3*$^+$).

Gene Disruption

The *pof3*$^+$ gene was disrupted using polymerase chain reaction (PCR)-generated fragments as described (Bähler *et al.*, 1998). A whole ORF was deleted and replaced with the *ura4*$^+$ gene in a diploid. At least 20 asci were dissected for each strain. In the case of disruption by the *kan*^{r} gene, a haploid strain was used directly to disrupt *pof3*$^+$.

UV Irradiation and Detection of Thymine Dimers

Approximately 10^9 cells of wild-type or *pof3* mutants were collected on filter papers (HAWG025; Millipore, Bedford, MA) and irradiated with UV (100 J/m^2, UV Stralinker 1800; Stratagene, La Jolla, CA). Cells on filters were resuspended in rich liquid medium and aliquots were collected afterward for immunoblotting. Genomic DNA was isolated from each sample, spotted on nitrocellulose paper, and fixed as described (McCready *et al.*, 1993). To detect thymine dimers, monoclonal antibody specific to cyclobutane pyrimidine dimer (TDM-2) (Mori *et al.*, 1991) was used. For a loading control, duplicate samples were spotted onto Parafilm (American National Can, Neenah, WI) and stained with ethidium bromide.

Mitotic Chromosome Stability Test

Standard procedure for measurements of nonessential minichromosomes (Ch10-CN2) (Niwa *et al.*, 1989) was followed (Allshire *et al.*, 1995). Briefly cells (500–1000) from Ade$^+$ colonies were plated on YE plates and incubated at 30°C for 4 d. Some plates were further incubated for 2 d at 4°C to allow development of the red color in Ade$^-$ colonies. The number of colonies with a red sector covering at least half of the colonies was counted. The number of chromosome loss events per division is the number of these half-sectored colonies divided by the total number of white colonies plus half-sectored colonies.

Chromosomally Integrated Epitope Tagging

The N- and C-terminal epitope tagging of the *pof3*$^+$ gene was performed with PCR-generated fragments (Bähler *et al.*, 1998). Green fluorescent protein (GFP), triple hemagglutinin (3HA), and 13Myc epitopes were used. Whereas C-terminal tagging with HA and Myc under the natural promoter did not interfere with Pof3 function, GFP tagging at the C terminus was not functional, because strains containing Pof3-GFP showed cell elongation phenotypes like those of gene-deleted mutants. For N-terminal tagging, GFP under the control of the thiamine-repressible weak *nmt81* promoter was integrated in-frame in front of the initiator ATG of the genomic *pof3*$^+$ gene. This strain (*nmt81-GFP-pof3*$^+$) grew apparently normally irrespective of the presence or absence of thiamine. It ap-

Table 1. Strain list

Strains	Genotype	Derivations
HM123	*h⁻leu1*	Our stock
TP108-3A	*h⁻leu1ura4*	Our stock
mik1	*h⁻leu1ura4mik1::LEU2*	Paul Nurse
wee1-50	*h⁻leu1ura4wee1-50*	Paul Nurse
mik1wee1	*h⁻leu1ura4mik1::LEU2wee1-50*	Paul Nurse
rad1-d	*h⁺leu1ura4rad1::ura4⁺*	Anthony M. Carr
rad3-d	*h⁺leu1ura4rad3::ura4⁺*	Anthony M. Carr
rad3^{ts}	*h⁺leu1ura4ura4rad3-ts*	Anthony M. Carr
rad17-d	*h⁻leu1ura4ade6rad17::ura4⁺*	Anthony M. Carr
rad26-d	*h⁻leu1ura4ade6rad26::ura4⁺*	Anthony M. Carr
chk1	*h⁻leu1ura4ade6chk1::ura4⁺*	Anthony M. Carr
crb2	*h⁻leu1ura4crb2::ura4⁺*	(Saka *et al.*, 1997)
cds1	*h⁻leu1ura4cds1::ura4⁺*	(Murakami and Okayama, 1995)
AE148	*h⁻leu1ura4mad2::ura4⁺*	(Kim *et al.*, 1998)
Δatb2	*h⁻leu1atb2::LEU2*	(Adachi *et al.*, 1986)
CN2	*h⁻leu1ade6-704Ch10-CN2*	(Niwa *et al.*, 1989)
1872	*h^{90}leu1ura4-DS/Eade6-210his3-d1 otr1(SphI)::ade6⁺ura4⁺-tel2L*	Robin C. Allshire
TP487-5C	*h⁻leu1ura4pof3::ura4⁺mik1::LEU2*	This study
TP487-14B	*h⁻leu1ura4pof3::ura4⁺mik1::LEU2wee1-50*	This study
TP492-9B	*h⁻leu1ura4pof3::ura4⁺*	This study
SKP414-17	*h⁻leu1ura4pcu1⁺-13myc-kan^r*	(Osaka *et al.*, 2000)
SKDP521	*h⁻/h⁺leu1/leu1ura4/ura4his7/his7 ade6-210/ade6-216pof3::ura4⁺/+*	This study
SKPNX01	*h⁻leu1ura4pof3::ura4⁺wee1-50*	This study
SKP459	*h⁻ura4 pof3::ura4⁺rad3^{ts}*	This study
SKP465	*h⁻leu1ura4kan^r-nmt81-GFP-pof3⁺*	This study
SKP467-13	*h⁻leu1ura4chk1⁺-13myc-kan^r*	This study
SKP470	*h⁻leu1ura4pof3::kan^{r}cut12⁺-GFP-ura4⁺*	This study
SKP471	*h⁻leu1ura4pof3::kan^r*	This study
SKP472	*h⁻leu1ura4pof3::ura4⁺chk1⁺-13myc-kan^r*	This study
SKP481-1	*h⁻leu1ura4pof3::kan^{r}mad2::ura4⁺*	This study
SKP491	*h⁻leu1ade6-704pof3::kan^{r}Ch10-CN2*	This study
SKP494	*h^{90}leu1ura4-DS/Eade6-210his3-d1pof3::kan^r otr1(SphI)::ade6⁺ura4⁺-tel2L*	This study
SKP512	*h⁻leu1ade6pof3⁺-13myc-kan^r*	This study
SKP513-1B	*h⁻leu1ura4 pof3::kan^{r}cds1::ura4⁺*	This study
SKP524	*h⁻leu1ura4cdc25-22pof3⁺-13myc-kan^r*	This study
SKP525	*h⁻leu1ura4pof3⁺-3HA-kan^{r}pcu1⁺-13myc-kan^r*	This study

All the *leu1* and *ura4* alleles used in this study are *leu1-32* and *ura4-D18*, respectively, unless otherwise stated.

peared that the small amount of GFP-Pof3 protein produced under repressed conditions was sufficient to support normal growth. The *chk1⁺* gene was tagged in its C terminus with 13Myc in wild type and *pof3* mutants.

Synchronous Culture

Exponentially growing *cdc25-22* mutant carrying the tagged *pof3⁺* gene (*pof3⁺-13myc*) was first arrested at 35.5°C for 4 h and 15 min and then shifted back to 26°C. Aliquots were taken every 20 min until 340 min. To monitor synchrony, the percentage of septated cells was counted using Calcofluor to stain the septum.

Live Imaging of GFP-Pof3 and Chromosomal DNA

Exponentially growing cells containing integrated *nmt81-GFP-pof3⁺* were washed with distilled water and resuspended in water. Chromosomal DNA was stained with Hoechst 33342 (1 μg/ml) (Chikashige *et al.*, 1994). GFP-Pof3 and chromosomal DNA were visualized by fluorescence microscopy.

Immunochemical Assays

Fission yeast whole cell extracts were prepared using glass beads to disrupt yeast cells in TEG buffer (50 mM Tris-HCl, pH 7.5, 1 mM EDTA, 10% glycerol, 30 mM NaCl, 1 mM dithiothreitol, 60 mM β-glycerophosphate, 15 mM *p*-nitrophenylphosphate, 0.1 mM NaF, 10 μg/ml soybean trypsin inhibitor, 20 μg/ml leupeptin, 50 μg/ml aprotinin, 2 μg/ml pepstatin, 1 mM phenylmethylsulfonyl fluoride, 0.1 mM Na-orthovanadate). Mouse monoclonal anti-α-tubulin antibody (TAT-1) was provided by Dr. Keith Gull (University of Manchester, Manchester, UK). Mouse monoclonal anti-HA (16B12), anti-Myc (9E10) antibodies, rabbit polyclonal anti-HA (HA.11) and anti-Myc antibodies were purchased from BAbCO (Richmond, CA). Rabbit polyclonal anti-Skp1 antibody was prepared as follows. cDNA containing an entire *skp1⁺* ORF was amplified using fission yeast cDNA library (CLONTECH, Palo Alto, CA) as a template with PCR and cloned into pET-14b (Novagen, Madison, WI). 6His-tagged Skp1 fusion protein was purified by Ni^{2+}-NTA beads (QIAGEN, Valencia, CA) as recommended by the supplier. Crude anti-Skp1 serum was affinity purified using the Skp1 fusion protein that was

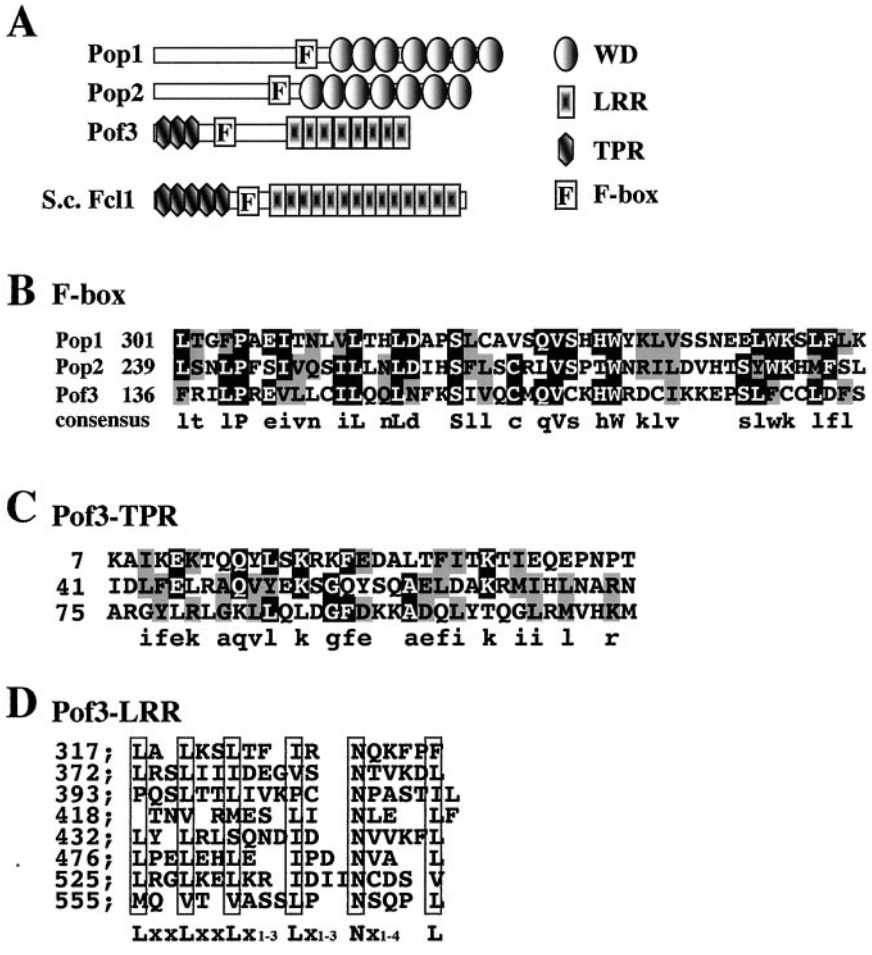

Figure 1. Structure of the Pof3 F-box protein. (A) Overall structural organization. Schematic comparison of Pof3 and three other F-box proteins (fission yeast Pop1 and Pop2 and budding yeast Fcl1) is depicted. F in squares shows the F-box, whereas three other protein–protein interaction domains are indicated as follows: WD-repeats (ovals), TPR (squares), and LRRs (hexagons). (B and C) Alignment of amino acid sequence of the F-box (B) and TPR (C). Identical amino acids are shown in black squares with open letters, whereas conservative amino acids are shown in dark squares with black letters. Amino acid number and consensus amino acid residues are shown to the left and at the bottom, respectively. (D) Sequence alignment of LRRs. Consensus amino acid residues are boxed, and a repeating unit is shown below with consensus leucine and asparagine residues.

immobilized on nitrocellulose filters. Horseradish peroxidase-conjugated goat anti-rabbit IgG, goat anti-mouse IgG (Bio-Rad, Hercules, CA), and a chemiluminescence system (enhanced chemiluminescence; Amersham plc, Little Chalfont, Buckinghamshire, United Kingdom) were used to detect bound antibody. For immunoprecipitations, 2 mg of total protein extract was used (Katayama *et al.*, 1999). To detect phosphorylation of Chk1-13Myc by immunoblotting, 10% SDS polyacrylamide gel in which a ratio between acrylamide and bis is 200:1 was used.

Fluorescence Microscopy

Cells were fixed with methanol or formaldehyde and images of GFP, 4,6-diamidino-2-phenylindole (DAPI), or Hoechst 33342 were observed by fluorescence microscopy connected to a chilled video-linked charge-coupled device camera (model C5985; Hamamatsu, Bridgewater, NJ). Images were processed by use of Adobe Photoshop (version 5.5; Adobe Systems, Mountain View, CA).

Measurements of Telomere Length

Genomic DNA was prepared from wild type and *pof3* mutants, digested with *Apa*I or *Eco*RI, run on a 1.2% agarose gel, and blotted onto nitrocellulose filters. Southern hybridization was performed with telomere probes (Sugawara and Szostak, 1986; Hiraoka *et al.*, 1998) as previously described (Cooper *et al.*, 1997). A nonradioisotopic detection system (enhanced chemiluminescence direct nucleic acid labeling system; Amersham plc) was used.

RESULTS

Structure of Pof3 F-box Protein

By searching the fission yeast genome database with the F-box sequence as a query, we have identified 15 ORFs, which encode putative F-box proteins. These include the *pop1*$^+$ and *pop2*$^+$ genes, which we had identified previously in an independent study, as those encoding components of the SCF ubiquitin ligase (Kominami and Toda, 1997; Kominami *et al.*, 1998). Besides these two genes, all 13 other ORFs are novel and designated *pombe* F-box proteins (*pof1*$^+$ to *pof13*$^+$; Figure 1, A and B). In addition to the conserved F-box domain, F-box proteins often contain, usually in their C-terminal region, a protein–protein interaction motif, e.g., Pop1 and Pop2 both contain WD-repeat motifs (Kominami and Toda, 1997; Kominami *et al.*, 1998). Domain searching showed that the Pof3 protein is unique in that, besides the F-box, it is composed of two separate protein–protein interaction domains (Figure 1A). One is three repeats of a tetratricopeptide repeat (TPR) motif (Goebl and Yanagida, 1991) that locates to the N-terminal region proximal to the F-box

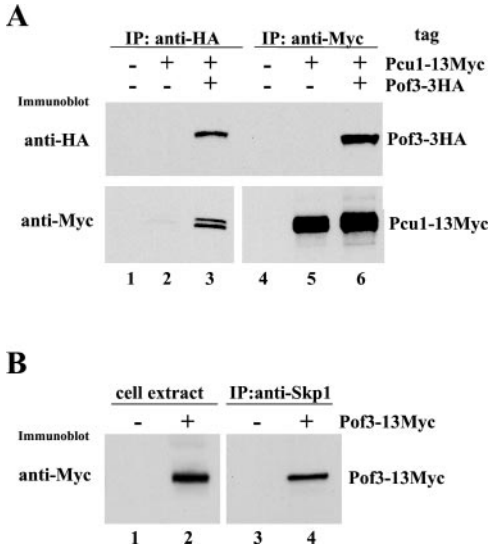

Figure 2. Complex formation between Pof3 and core components of the SCF ubiquitin ligase. (A) Interaction between Pof3 and cullin-1. Protein extracts were prepared from untagged wild-type (TP108-3A; Table 1, lanes 1 and 4), a singly tagged (SKP414-17, *pcu1*$^+$*-13myc*, lanes 2 and 5), or doubly tagged strain (SKP525, *pof3*$^+$*-3HA pcu1*$^+$*-13myc*, lanes 3 and 6), and immunoprecipitation was performed with anti-HA (lanes 1–3) or with anti-Myc antibody (lanes 4–6). After running on SDS-PAGE, immunoblotting was performed with anti-HA (top) or anti-Myc antibody (bottom). (B) Interaction between Pof3 and Skp1. Protein extracts were prepared from untagged wild-type (lanes 1 and 3) or a Pof3-13Myc strain (SKP512, lanes 2 and 4), and immunoprecipitation was performed with anti-Skp1 antibody (lanes 3 and 4), followed by immunoblotting with anti-Myc antibody. Total extracts were also run (lanes 1 and 2).

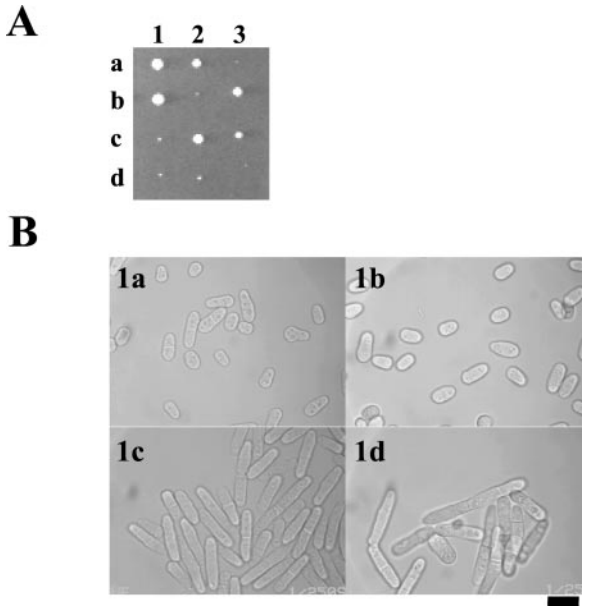

Figure 3. Gene disruption of *pof3*$^+$ results in cell elongation and cell cycle delay. (A) Tetrad analysis of diploid heterozygous for *pof3*. Three tetrads dissected from heterozygous diploid (SKDP521) are shown. In each tetrad, two normal-sized and two small-sized colonies are formed, of which small colonies are *pof3* deleted. (B) Cell morphology of Δ*pof3* cells. Cells taken from one set of tetrads (A, 1a–d) were grown on rich media plates for 1 d. Bar, 10 μm.

(residues 7–108; Figure 1C), whereas the other is eight repeats of a leucine-rich-repeat motif (LRR) (Kobe and Deisenhofer, 1994), which is situated in the C-terminal region (residues 317–569; Figure 1D).

A homology search by using Pof3 as a query against the entire database (DDBJ, EMBL, GenBank, and SWISS-PLOT) showed that budding yeast contains an analogous F-box protein, Fcl1/Dia2 (Figure 1A).

Pof3 Is a Component of SCF Ubiquitin Ligase

The F-box is a binding module for Skp1 (Bai *et al.*, 1996), a universal component of the SCF ubiquitin ligase (Feldman *et al.*, 1997; Skowyra *et al.*, 1997). However, recent analysis has shown that there are F-box proteins that are, despite binding to Skp1, neither components of the SCF nor involved in SCF activity (Kaplan *et al.*, 1997; Galan *et al.*, 2001; Reimann *et al.*, 2001; Seol *et al.*, 2001). To clarify whether Pof3 functions via fission yeast SCF, binding between Pof3 and known components of SCF was examined. For this purpose, strains in which the chromosomal *pof3*$^+$ gene was tagged with 3HA or 13Myc were constructed (Bähler *et al.*, 1998). Also a double-tagged strain (Pof3–3HA Pcu1-13Myc) was constructed using a tagged Pcu1 strain (Pcu1 is a cullin-1 homolog) (Kominami *et al.*, 1998). Tagging did not interfere with protein function because growth rate of these strains is indistinguishable compared with wild-type cells.

Reciprocal immunoprecipitation was performed using anti-HA and anti-Myc antibodies. Immunoblotting showed that anti-HA coprecipitated Pcu1-13Myc and conversely anti-Myc coprecipitated Pof3-3HA (Figure 2A). We have previously shown that the Pcu1 protein consists of two populations, one is modified by NEDD8 and the other is unmodified (Osaka *et al.*, 2000). Pof3-3HA coprecipitated with two bands of Pcu1-13Myc (lane 3), suggesting that both forms of Pcu1, unmodified and modified by NEDD8, are capable of forming a complex with Pof3. It is of note that in the case of Pop1, only the modified form of Pcu1 forms a complex with Pop1 in vivo (Osaka *et al.*, 2000). To confirm binding of Pof3 to the SCF, immunoprecipitation was performed with anti-Skp1 antibody (in this case, a Pof3-13Myc strain was used) and immunoblotted with anti-Myc antibody. As shown in Figure 2B, Pof3-13Myc forms a complex with Skp1. From these results, we concluded that the novel F-box protein Pof3 is a component of the SCF ubiquitin ligase.

Loss of Pof3 Results in Cell Cycle Delay during G2 Phase

To examine the role of Pof3, gene disruption was performed, in which the complete ORF of one of the *pof3*$^+$ genes in a diploid cell was deleted. Tetrad dissection of this heterozygous diploid showed that the *pof3*$^+$ gene was not essential for cell viability, but *pof3*-deleted haploid cells (Δ*pof3*) grew

Table 2. Genetic interaction between *pof3* and *wee1* and *mik1*

Strains	Cell length at division (μm)	
	26°C	36°C
Wild type	14.0 ± 1.3	14.3 ± 1.3
mik1::LEU2	13.6 ± 1.5	13.7 ± 1.5
wee1-50	11.1 ± 2.1	8.0 ± 1.2
wee1-50mik1::LEU2	10.6 ± 1.2	lethal
pof3::ura4+	24.2 ± 4.1	36.2 ± 10.9
pof3::ura4+mik1::LEU2	23.3 ± 3.6	38.9 ± 14.3
pof3::ura4+wee1-50	22.1 ± 3.7	15.7 ± 2.7
pof3::ura4+wee1-50mik1::LEU2	14.5 ± 0.8	lethal

The length of at least 100 septated cells was measured in each strain.

Table 3. Synthetic lethal interaction between *pof3* and checkpoint mutants

Double mutants	Phenotype
pof3::ura4+ Δ*rad1*	lethal
Δ*rad3*	lethal
rad3ts	ts
Δ*rad17*	lethal
Δ*rad26*	lethal
Δ*chk1*	lethal[a]
Δ*crb2*	lethal
Δ*cds1*	slow growth[b]
Δ*mad2*	viable[c]

[a] Small pin colonies were sometimes formed, but these colonies were unable to propagate.

[b] Doubling time of this double mutant at 30°C is approximately 50% longer than a *pof3* single mutant.

[c] Colony size is indistinguishable from a Δ*pof3* single mutant.

much slower (the doubling time is ~180 min at 30°C compared with 130 min for wild-type cells; Figure 3A). Morphological observation showed that *pof3*-deleted cells exhibited cell elongation, reminiscent of a G2 cell cycle delay (Figure 3B). Average cell length at division was 24 μm at 26°C and division delay was exaggerated when grown at 36°C (36 μm, whereas it was 14 μm in wild-type cells at both temperatures; Table 2).

Next, genetic analysis was performed using various cell cycle mutants to examine the involvement of Pof3 in cell cycle progression. It was found that G2 delay phenotypes of *pof3* mutants were independent of Wee1 and Mik1, negative regulators of Cdc2 (Nurse, 1990), mutants of Δ*pof3wee1-50* (at 26 or 36°C) or Δ*pof3*Δ*mik1wee1-50* (at 26°C) divided at a size intermediate between each single mutant (Table 2). Also *pof3*-dependent cell cycle delay was synergistic with *cdc25-22* mutants (Katayama and Toda, unpublished data), defective in a phosphatase that positively regulates Cdc2. This result suggested that Pof3 is involved in cell cycle transition from G2 to M phase, and indirectly, positively regulates Cdc2.

pof3 Mutants Activate DNA Damage Checkpoint

We were interested in seeking further for the molecular mechanisms underlying G2 delay phenotypes in the *pof3* mutant. One possibility was that in the *pof3* mutant, the DNA structure checkpoint, which is operational at the G2/M transition (Carr and Hoekstra, 1995; Russell, 1998), is somehow activated under vegetative growing conditions. To address this question, a series of genetic crosses between Δ*pof3* and checkpoint mutants were performed. The results are outlined below and also summarized in Table 3. It was found that Δ*pof3* was lethal in combination with a number of checkpoint mutants, including deletion alleles of *rad1+*, *rad3+*, *rad17+*, and *rad26+*, which are the initial components of the DNA structure checkpoint (Carr and Hoekstra, 1995; Russell, 1998). To characterize the terminal phenotypes of *pof3* mutants in the absence of checkpoint function, Δ*pof3* was crossed with a temperature-sensitive *rad3* strain (*rad3ts*) (Mundt *et al*., 1999). In line with previous analysis using *rad3*-deleted strains, Δ*pof3rad3ts* double mutants were viable at 26°C, but could not form colonies at 36°C (Figure 4A). Liquid culture analysis showed that a Δ*pof3rad3ts* strain lost viability rapidly upon temperature shift-up (Figure 4B). Nuclear staining with DAPI showed that this double mutant lost viability because of "cut" phenotypes, septum formation without nuclear division, characteristic of checkpoint defects (Figure 4C, arrowheads) (Enoch *et al*., 1992). It should be noted that in a single Δ*pof3* strain, cells with defects in chromosome segregation were observed (see below; Figure 6, B and C, arrows). From these results, we concluded that in the absence of Pof3 the DNA structure checkpoint is activated.

The DNA structure checkpoint is a bifurcated pathway in which one branch responds to stalled DNA replication, whereas the other responds to DNA damage. To distinguish in which pathway Pof3 is involved, crosses between Δ*pof3* and Δ*chk1* or Δ*cds1* were performed. These two genes encode protein kinases that act downstream of the aforementioned checkpoint Rad proteins. The Chk1 kinase is involved in the DNA damage checkpoint, whereas Cds1 is required for the DNA replication checkpoint (Murakami and Nurse, 2000; Rhind and Russell, 2000). Δ*pof3* was synthetic lethal with Δ*chk1*, but not with Δ*cds1*, although growth of Δ*pof3*Δ*cds1* mutants was compromised (Table 3). This result suggested that in the absence of Pof3, the DNA damage checkpoint is activated. This notion was further supported by synthetic lethality between Δ*pof3* and the Δ*crb2*/Δ*rhp9* mutant (Table 3), which is, like Δ*chk1*, involved in the DNA damage checkpoint, but not in the DNA replication checkpoint (Saka *et al*., 1997; Willson *et al*., 1997; Esashi and Yanagida, 1999). Therefore, Pof3 plays a crucial role in cellular surveillance mechanism of DNA damage such that in its absence the DNA damage checkpoint is activated, which results in G2 cell cycle delay.

In pof3 Mutants, Chromosomal DNA Is Damaged

Having established that G2 cell cycle delay in the absence of Pof3 is ascribable to activation of the DNA damage checkpoint, we next asked what is the molecular basis of this activation. To explain this phenotype, two scenarios are readily predictable. One is that in *pof3* mutants DNA is physically damaged as in the case of UV irradiation,

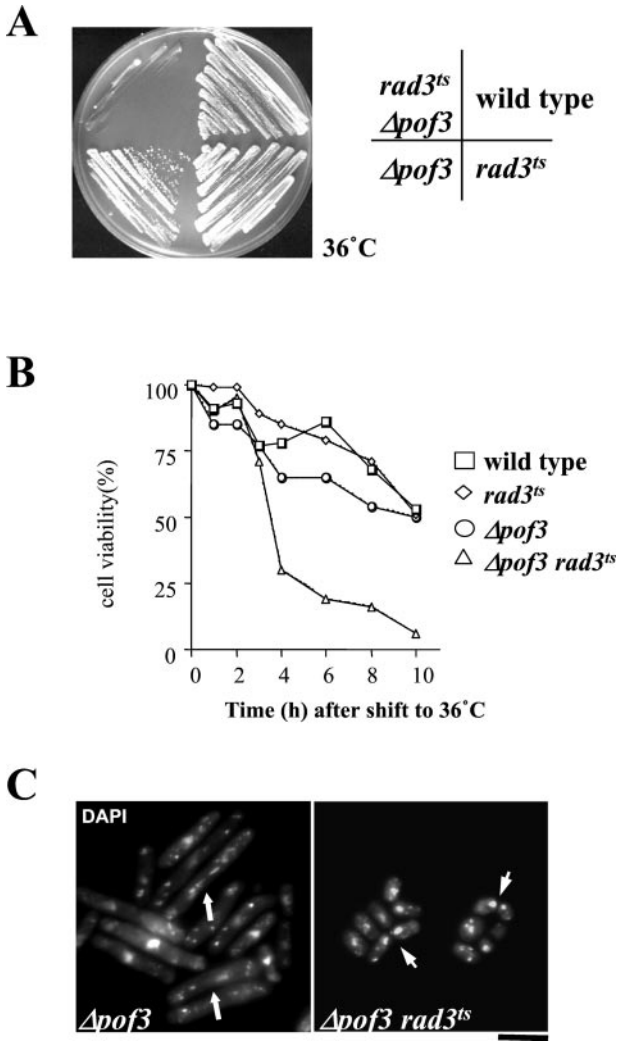

Figure 4. DNA damage checkpoint is activated in the absence of Pof3. (A) Synthetic lethality between Δ*pof3* and ts *rad3* mutants. Cells of wild-type (HM123), *rad3*^{ts}, Δ*pof3* (SKP471), or Δ*pof3rad3*^{ts} (SKP459) were streaked on rich media plates and incubated at 36°C for 2 d. (B) Loss of viability in Δ*pof3rad3*^{ts}. Exponentially growing cultures of four strains shown in A (wild type, squares; *rad3*^{ts}, diamonds; Δ*pof3*, circles; Δ*pof3rad3*^{ts}, triangles) were shifted from 26 to 36°C. Cell number was measured at each time point and viability was examined by plating cells on rich media plates after appropriate dilution. After incubating plates at 26°C, the number of colonies was counted and viability was calculated by dividing the number of viable colonies by the cell number. (C) Checkpoint defective phenotypes of Δ*pof3rad3*^{ts}. Cells of Δ*pof3* (left) or Δ*pof3rad3*^{ts} (right) grown at 26°C were shifted to 36°C, and incubated for 3 h, and nuclear DNA was stained with DAPI. Arrowheads show cut cells, whereas arrows emphasize cells with defects in chromosome segregation (see text; Figure 6, B and C). Bar, 10 μm.

whereas the other possibility is that downstream components are activated without any DNA damage, such as overproduction of the Chk1 kinase (Furnari *et al.*, 1997).

To clarify this point, immunoblotting against DNA was performed with a monoclonal antibody specific to thymine dimers (TDM-2) (Mori *et al.*, 1991). As a control, wild-type and Δ*pof3* cells were also treated with UV. In wild-type cells, there were no thymine dimers present under exponentially growing conditions (−UV; Figure 5A, top), whereas upon UV irradiation, their formation was easily detected with immunoblotting (+UV). Thymine dimers were sustained for 1 h after irradiation then DNA repair occurred and they almost disappeared after 2 h. In contrast, in *pof3* mutants, small but significant amounts of thymine dimers existed in growing cultures (Figure 5A, bottom), suggesting that without adverse treatment, chromosomal DNA of *pof3* mutants has already suffered from some sort of DNA damage. It should be noted that, although thymine dimers were formed without treatment, their amount was increased dramatically with UV irradiation like wild type, and more importantly these newly formed dimers were repaired with almost the same kinetics as wild-type cells. As a result, after 4 h a similar amount of residual thymine dimers to that found before irradiation was detectable in the mutant. This indicates that the repair machinery itself is not impaired in the *pof3* mutant.

It is known that DNA damage induces phosphorylation of the Chk1 kinase, which is detectable as a slower mobility band on SDS-polyacrylamide gel (Walworth and Bernards, 1996). To examine whether Chk1 is already phosphorylated in *pof3* mutants without any exogenous damage, the chromosomal *chk1*$^{+}$ gene was tagged with 13Myc in wild-type and *pof3* backgrounds. Protein extracts were prepared before and after UV irradiation, and immunoblotting performed with anti-Myc antibody. As shown in Figure 5B, it was found that Chk1 is phosphorylated in the *pof3* mutant, a slower mobility band was detected in exponentially growing *pof3* cells (lane 4), whereas in wild-type cells this form only appeared upon UV irradiation (lane 3). These results established that in the *pof3* mutant, chromosomal DNA is damaged constitutively, which induces activation of the DNA damage checkpoint pathway.

If *pof3* mutants suffer from DNA damage, they would be expected to be hypersensitive to further damage. This was indeed the case. As shown in Figure 5C, compared with wild type, Δ*pof3* cells were more sensitive to UV irradiation. This hypersensitivity was not due to checkpoint defects, because *pof3* mutant cells showed, like wild-type cells and unlike *rad3* mutants, cell elongation upon treatment with phleomycin (Figure 5D). This drug is known to induce single- and double-stranded breaks and leads to activation of the DNA damage checkpoint (Steighner and Povirk, 1990; Belenguer *et al.*, 1995; Wang *et al.*, 1999). On the other hand, *pof3* mutants were not hypersensitive to hydroxyurea (HU; Figure 5E), and also the process of DNA replication appeared normal, because a G2 peak appeared in a similar kinetic to wild-type cells when nutrient-derived G1 cells were released into the rich medium (Katayama and Toda, unpublished data). Taking these results together, we propose that Pof3 plays a role in the maintenance of genome integrity and its absence results in DNA damage, including formation of thymine dimers and leads to Chk1 phosphorylation and G2 cell cycle delay even under normal growing conditions.

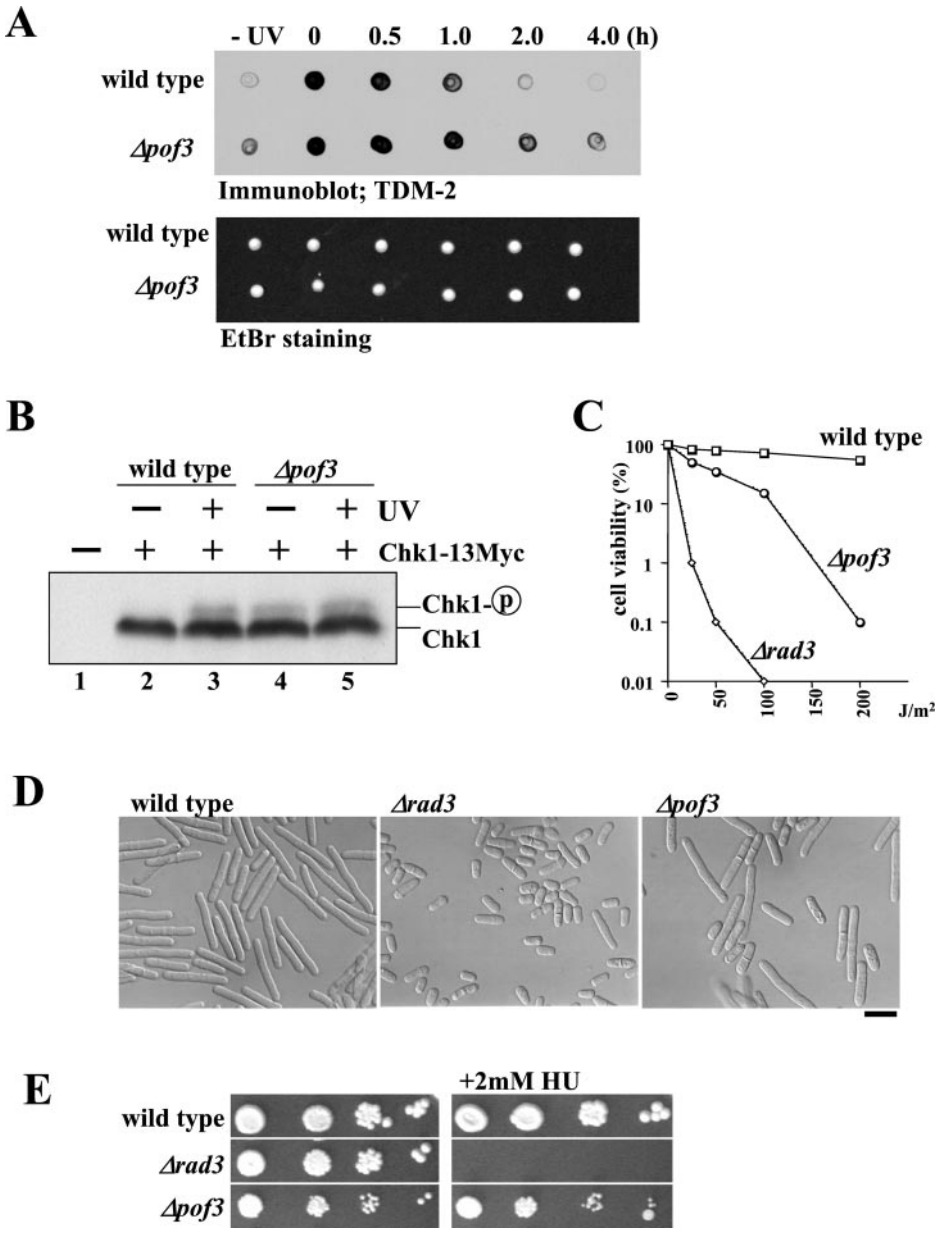

Figure 5. DNA is damaged in *pof3* disruptants. (A) Detection of thymine dimers. Wild-type and Δ*pof3* cells collected on filter papers were irradiated with UV (100 J/m^2) and resuspended in fresh liquid medium at 26°C. Genomic DNA was prepared before and after UV irradiation (up until 4 h) and blotted onto a nitrocellulose filter (top) and also onto parafilm (bottom). The filter was immunoblotted with specific anti-thymine dimer antibody (TDM-2) (Mori *et al.*, 1991), whereas DNA spotted on Parafilm (bottom) was stained with ethidium bromide (ETBr) to ensure equal loading of DNA. (B) Phosphorylation of Chk1. Wild-type (SKP467-13, lanes 2 and 3) and Δ*pof3* cells (SKP472, lanes 4 and 5) tagged with Chk1-13Myc were grown exponentially and collected on two nitrocellulose filters. One filter of each strain was irradiated with UV (100 J/m^2). After 20-min incubation in rich liquid medium for recovery, protein extracts were prepared from with (lanes 3 and 5) and without irradiation (lanes 2 and 4) and immunoblotting was performed with anti-Myc antibody. Immunoblotting was also performed in extracts from a nontagged wild-type strain (lane 1) as a negative control. Bands corresponding to phosphorylated (top) and nonphosphorylated Chk1 are marked. (C) Hypersensitivity to UV. The three strains indicated (wild-type, squares; Δ*rad3*, diamonds; Δ*pof3*, circles) were plated on rich medium and irradiated with various doses of UV. The number of viable colonies was counted after 4-d incubation at 26°C. Vertical axis (%) is shown logarithmically. (D) Normal responses to DNA damage in Δ*pof3*. The three strains indicated were grown in rich liquid culture in the presence of phleomycin (10 μg/ml) at 26°C for 5 h, and cell morphology was observed. Bar, 10 μm. (E) Normal sensitivity to HU. Cells of wild-type, Δ*rad3* or Δ*pof3* were spotted onto rich media plates in the presence (right) or absence (left) of 2 mM HU, as serial dilutions (~10^5 cells in the left row in each lane and then diluted 10-fold in the subsequent rightward spots) and incubated at 30°C for 3 d.

pof3 Mutants Show High Frequency of Minichromosome Loss with Impaired Chromosome Segregation

Given that Pof3 is required for genome integrity, we now questioned whether Pof3 is involved in chromosome segregation. To this end, we first examined chromosome stability in *pof3* mutants. Using a standard minichromosome assay (Niwa *et al.*, 1989), the frequency of minichromosome loss was examined. As shown in Figure 6A, red colonies of adenine auxotroph were readily detectable in *pof3* mutants. Quantitative measurement of the rate of loss indicated that *pof3* mutants lose minichromosomes at least 500-fold higher at frequency than wild-type cells (Figure 6A, right).

Second, we examined more carefully segregation patterns of endogenous chromosomes by live staining with Hoechst 33342 (Chikashige *et al.*, 1994). Although not extremely frequent, aberrantly segregating chromosomes were evident in some populations of mitotic *pof3* mutants (Figure 6B, 20–25% of mitotic cells). To examine their phenomenon in greater detail, a strain, which contained integrated *cut12*$^+$-*GFP* (*cut12*$^+$ encodes an integral component of the spindle pole body) (Bridge *et al.*, 1998), was constructed in a Δ*pof3* background, and anaphase cells were observed. What we found through this observation was abnormal mitotic cells with lagging chromosome, as shown in Figure 6C, similar to those reported in mutants defective in transcriptional silenc-

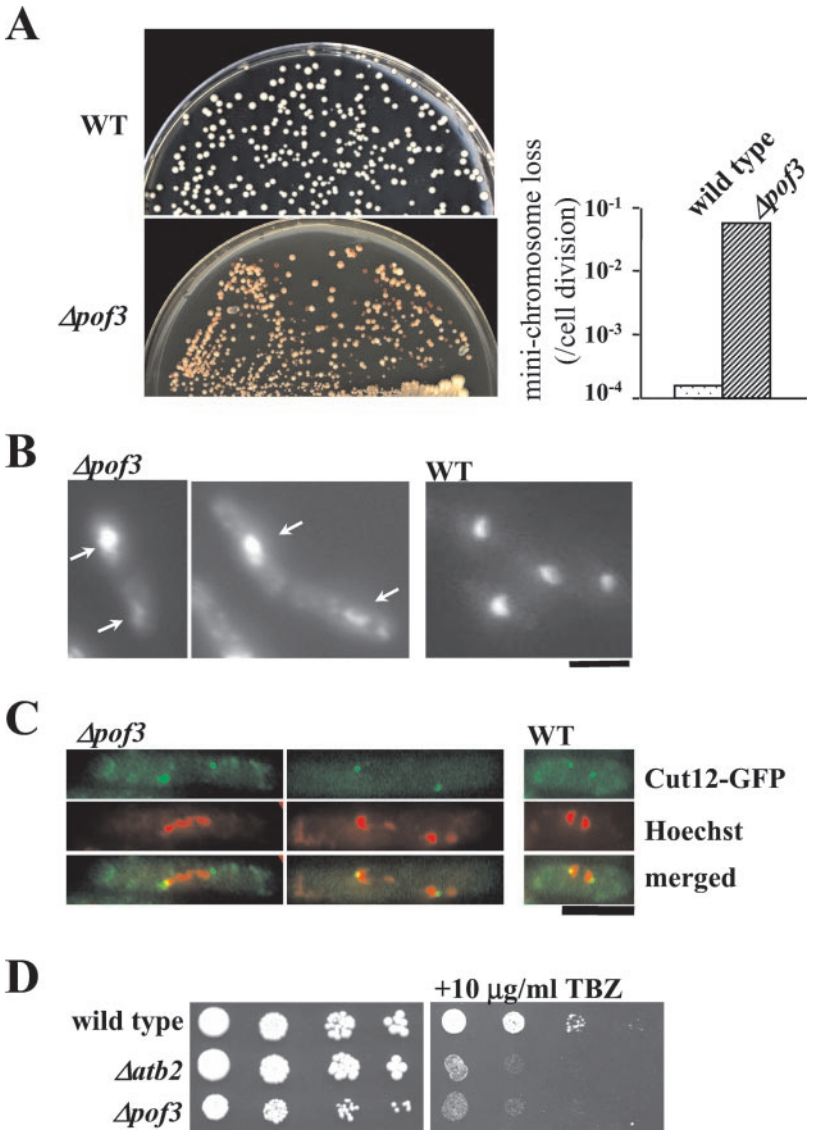

Figure 6. High frequency of minichromosome loss and chromosome segregation defects in the absence of Pof3. (A) Loss of minichromosomes. Wild-type (CN2, top) and Δ*pof3* cells (SKP491, bottom) containing minichromosomes, which had been grown in minimal medium without adenine (selective conditions for minichromosomes), were streaked on rich media plates and incubated at 30°C for 4 d (left). Colonies of adenine auxotroph appeared as red colonies. Quantification of chromosome loss rate is shown on the right-hand side. (B) Chromosome segregation defects. Exponentially growing Δ*pof3* was stained with Hoechst 33342. Unequally segregated chromosomes are marked with arrows. Wild-type control is shown on the right-hand side. (C) Visualization of lagging chromosome. Live cells of a wild-type or Δ*pof3* strain containing integrated *cut12*$^{+}$-*GFP* (green; Bridge *et al.*, 1998) are stained with Hoechst 33342 (red) and viewed by fluorescence microscopy to observe chromosomes and the spindle pole body. Bar, 10 μm. (D) Hypersensitivity to thiabendazole (TBZ). Cells of wild-type, Δ*pof3*, or Δ*atb2* (defective in α2-tubulin; Adachi *et al.*, 1986) strains were spotted onto rich media plates in the absence (left) or presence of thiabendazole (+TBZ, 10 μg/ml, right) as serial dilutions (~10^5 cells in the left row and then diluted 10-fold in each subsequent spot rightward) and incubated at 30°C for 3 d.

ing (Ekwall *et al.*, 1995, 1996; Pidoux *et al.*, 2000). Furthermore, consistent with these defective chromosome segregation and chromosome loss phenotypes, *pof3* mutants were hypersensitive to microtubule-destabilizing drugs (Figure 6D). Despite these defects, *pof3* mutants did not activate the kinetochore-mediated spindle assembly checkpoint, because growth properties of Δ*pof3*Δ*mad2* double mutants were indistinguishable from Δ*pof3* single mutants (Table 3). These results showed that Pof3 is required for faithful chromosome segregation and normal progression through anaphase.

Pof3 Localizes to Nucleus Continuously during Cell Cycle

Next, the cellular localization of the Pof3 protein was examined. GFP was tagged in the N terminus under thiamine-repressible weaker *nmt81* promoter (Basi *et al.*, 1993; Bähler *et al.*, 1998). This tagged strain grew normally in both the presence and the absence of thiamine. A series of live imaging of GFP-Pof3 costained with Hoechst 33342 are shown in Figure 7A. It was found that GFP-Pof3 localizes to the nucleus during the entire cell cycle. In addition to the chromatin region, Pof3 appeared to localize to nonchromatin region, because at anaphase, GFP signals were observed in not only chromatin regions but also interchromatin regions, the area between two segregating chromosomes (Figure 7A, c and d). The amount of Pof3 appeared to be constant during the cell cycle as shown in Figure 7B. G2-arrest *cdc25-22* block and release experiments indicated that Pof3-13Myc levels were not noticeably altered during the cell cycle. Taken together, these results showed that Pof3 is a nuclear protein, which may imply that Pof3 substrates are involved in DNA and chromatin integrity.

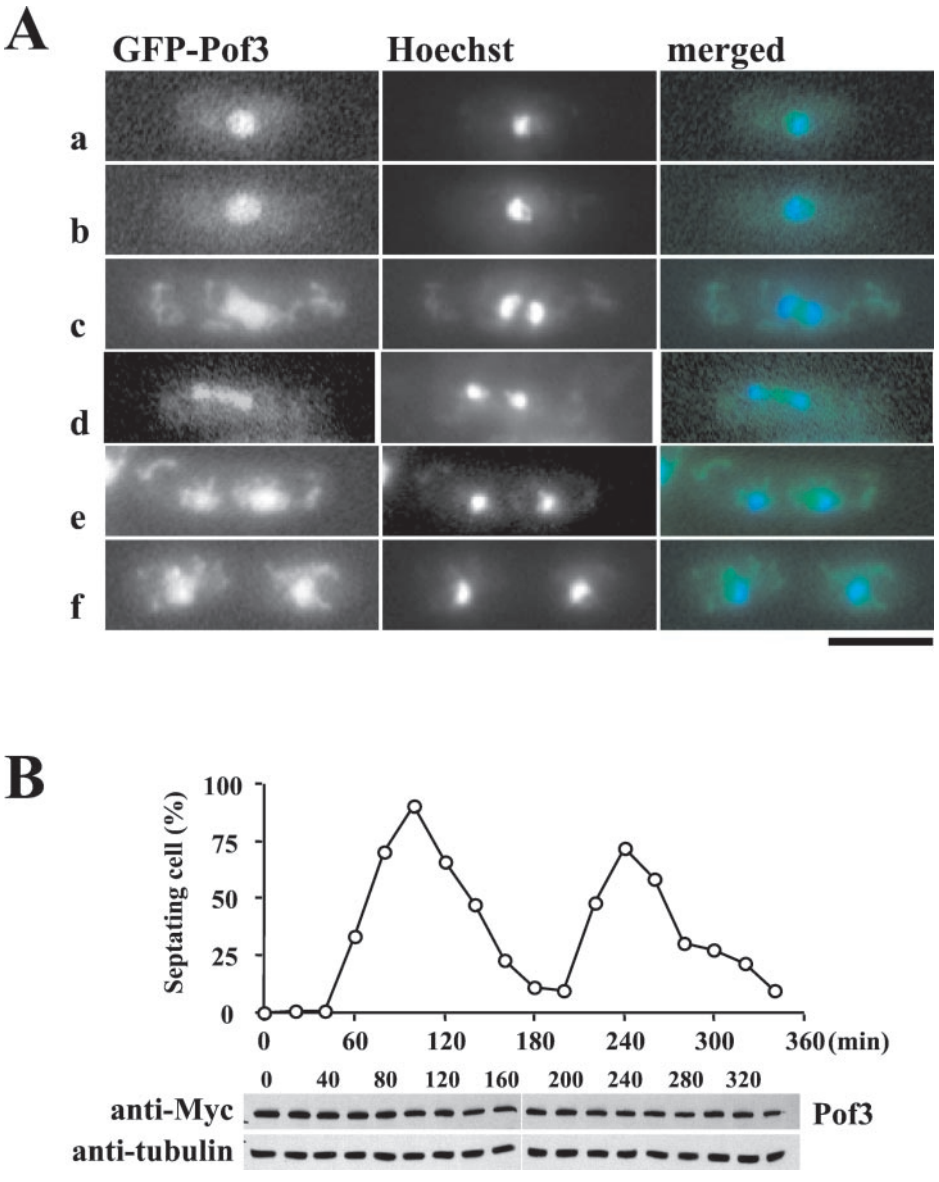

Figure 7. Nuclear localization of Pof3. (A) Pof3 localization during the cell cycle. A strain containing integrated *nmt81-GFP-pof3*$^+$ (SKP465) was grown in rich liquid medium and stained with Hoechst 33342. Representative images of cells in different cell cycle stages are shown (left, GFP-Pof3; middle, Hoechst 33342; right, merged). Bar, 10 μm. (B) Pof3 levels during the cell cycle. Exponentially growing *cdc25-22* mutants containing a tagged Pof3-13Myc (SKP524) was first arrested at 35.5°C for 4 h and 15 min, and shifted down to 26°C. Aliquots were taken every 20 min for immunoblotting and measurement of percentage of septated cells. α-Tubulin levels are used as a loading control.

Pof3 Is Required for Length Maintenance of and Silencing at Telomere

As mentioned previously, the abnormal chromosome segregation phenotypes are similar to those found in a series of mutants defective in the maintenance of chromatin structure (Ekwall *et al.*, 1995, 1996; Ekwall and Partridge, 1999; Pidoux *et al.*, 2000). It was reported that telomere architecture is tightly regulated via a complex genetic network in fission yeast as it is in other eukaryotes (Nakamura *et al.*, 1997; Dahlén *et al.*, 1998; Naito *et al.*, 1998; Matsuura *et al.*, 1999; Baumann and Cech, 2000, 2001; Manolis *et al.*, 2001), and in budding yeast *cdc13* mutants, which arrest at G2, are defective in telomere structure (Hartwell and Weinert, 1989). To examine whether Pof3 is involved in the maintenance of telomere integrity, telomere length was examined in this mutant. Southern hybridization analysis with telomere probes showed that telomere sequence is significantly shorter in this mutant (Figure 8, A and B). It should also be pointed out that, probably because of shorter telomeres, hybridization signals in telomere regions were reproducibly weaker in the *pof3* mutant (Figure 8B, lane 4).

It is known that, as in other eukaryotes, the fission yeast telomere is one of the heterochromatic DNA regions that shows position effect variegation, i.e., transcription of a gene inserted in this region is repressed (Nimmo *et al.*, 1994). This silencing is functionally linked to telomere structures because a number of mutants with defects in telomere length exhibit desilencing phenotypes (Cooper *et al.*, 1997; Dahlén *et al.*, 1998; Matsuura *et al.*, 1999). We were interested in whether Pof3 also plays a role in silencing at telomeres. A *pof3* mutant in which the *ura4*$^+$ gene is integrated in the telomere vicinity (Nimmo *et al.*, 1994) was constructed, and

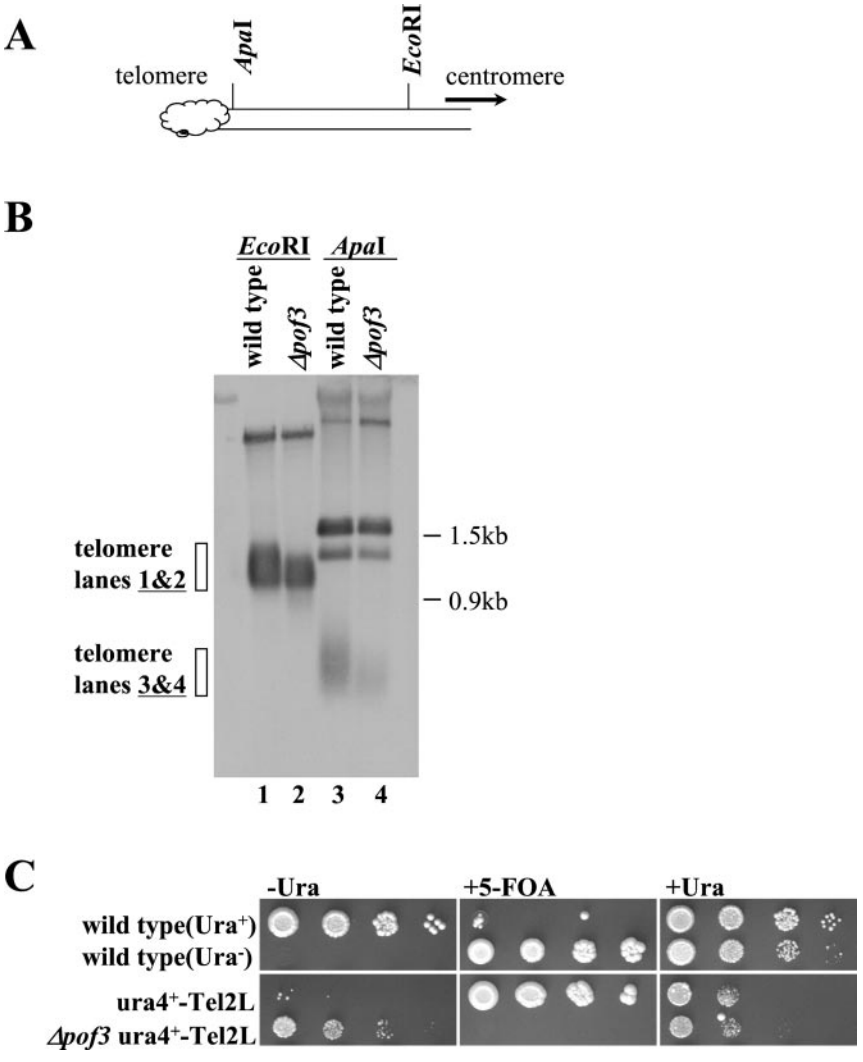

Figure 8. Pof3 is required for length maintenance and transcriptional silencing at the telomere. (A) Schematic depiction of the telomeric region of the chromosome. Two of the three chromosomes in fission yeast contain *Apa*I restriction sites just centromere-proximal to their telomeric repeats, whereas all three chromosomes contain *Eco*RI restriction sites at ~1 kb from the ends (Cooper *et al.*, 1997; Matsuura *et al.*, 1999). (B) Shortening of the telomere. Genomic DNA was prepared from exponentially growing wild-type (lanes 1 and 3) or Δ*pof3* cells (lanes 2 and 4), digested with *Eco*RI (lanes 1 and 2) or *Apa*I (lanes 3 and 4), run on a 1.2% agarose gel, transferred onto nylon membranes, and hybridized with specific telomeric sequences as a probe (Cooper *et al.*, 1997; Matsuura *et al.*, 1999). The telomere regions are marked with open rectangles. (C) Loss of silencing at the telomere. Four strains (Ura^+ and Ura^- control, wild-type, and Δ*pof3* strains, in which the *ura4*$^+$ marker gene is integrated in the telomeric region, 1872, and SKP494, respectively) were spotted in a serial dilution on minimal plates lacking uracil (left), rich media plates containing 1 mg/ml FOA, or minimal plates containing uracil.

the uracil requirement of this strain was examined. In contrast to a wild-type strain, which showed uracil auxotrophic phenotypes (Ura^-) and simultaneous resistance to 5′-fluoroorotic acid (FOA), *pof3* mutants were Ura^+ and also sensitive to FOA (Figure 8C). Therefore, the Pof3 F-box protein is required for silencing at the telomere and its length maintenance, in addition to chromosome stability and segregation.

DISCUSSION

In this study, we have shown that a novel F-box protein Pof3 plays an important role in genome integrity such that its absence results in a number of phenotypes, including cell cycle delay ascribable to activation of the DNA damage checkpoint, hypersensitivity to UV irradiation, chromosome instability, chromosome segregation defects, and telomere disfunction. As far as we are concerned, these types of abnormalities in genome integrity have not been described in any SCF mutants previously characterized, and we believe that our work sheds more light on the involvement of SCF-mediated proteolysis in cell proliferation and potentially in carcinogenesis.

Potential Substrates of SCF^{Pof3}

F-box proteins have been shown to play a role, as substrate-specific receptors, in the recruitment of substrates to specific sites for ubiquitination. For example, Cdc4 in budding yeast localizes to the nucleus, and this localization is essential for its substrate Far1 to be degraded (Blondel *et al.*, 2000). In this context, the nuclear localization of Pof3 suggests that substrates of SCF^{Pof3} are also nuclear proteins. Recent biochemical analysis shows further that a significant amount of Pof3 is fractionated as chromatin-bound forms (Katayama and Toda, unpublished data). It is possible that SCF^{Pof3} substrates are involved in chromatin architecture, and their accumulation in the *pof3* mutant results in some structural alterations in chromatin, including telomere regions, which are detected by the DNA damage checkpoint machinery.

pof3 disruptants show a number of defective phenotypes. Do these defects arise from the accumulation of a single protein or of multiple substrates, each of which results in distinct phenotypes? The activation of the DNA damage checkpoint and telomere disfunction might at least be attributed to a single cause. It is well known that abnormalities in the telomere lead to activation of this checkpoint. For instance, in budding yeast, mutations in a single-stranded, telomeric DNA binding protein, Cdc13, lead to G2 cell cycle arrest, ascribable to activation of the DNA damage checkpoint (Hartwell and Weinert, 1989). Furthermore, it has been shown that mutants defective in silencing at the telomere show chromosome segregation defects and a high frequency of minichromosome loss, like the *pof3* disruptant. These include mutations in the ATM/ATR homolog-encoding *tel1*$^+$ and *rad3*$^+$ (Matsuura *et al.*, 1999), the chromodomain protein-encoding *swi6*$^+$, the histone deacetylase-encoding *hda1*$^+$ and *hst4*$^+$ (Olsson *et al.*, 1998; Freeman-Cook *et al.*, 1999), and the histone H3 methyltransferase-encoding *clr4*$^+$ (Bannister *et al.*, 2001; Nakayama *et al.*, 2001a). It is, therefore, possible that the assorted phenotypes of the *pof3* mutant might arise from accumulation of a relatively small number of protein species. They could even be caused by accumulation of a single protein.

Accumulation of any inhibitory factors of these telomere/chromatin-associated proteins would lead to inactivation of function, resulting in defective phenotypes similar to those mentioned above. Thus, such inhibitory factors could be potential candidates for substrates for SCF^{Pof3}. Despite several efforts to determine proteins in *pof3* mutants with altered levels, at present none has been identified. It is intriguing that fission yeast Pof3 and budding yeast Fcl1 appear to play a similar role (Fcl1 stands for F-box/chromosome loss; Tyers, personal communication). It is highly likely that substrates for SCF^{Pof3} and SCF^{Fcl1} are conserved between these two yeast species, as in the case of SCF$^{Pop1,\ Pop2}$ and SCF^{Cdc4} (Toda *et al.*, 1999).

Lagging Chromosomes

Recent analysis in mammalian tissue culture cells has demonstrated that merotelic kinetochore orientation, which leads to lagging chromosomes, is a major mechanism of aneuploidy. Intriguingly, as in *pof3* or other fission yeast mutants mentioned above (*clr4*$^+$, *hst4*$^+$, *swi6*$^+$, etc.) (Pidoux *et al.*, 2000), these lagging chromosomes do not activate the Mad2-dependent spindle checkpoint, albeit exhibiting mitotic delay (Cimini *et al.*, 2001). Further analysis of the Pof3-dependent proteolysis pathway will enable us to shed light on the molecular mechanisms of this aneuploidy phenomenon.

Conserved Function of SCF^{Pof3} Ubiquitin Ligase

We have identified 15 F-box protein-encoding ORFs in the fission yeast genome, some of which are conserved throughout evolution, whereas others appear to exist only in yeast (budding and fission) or are orphan fission yeast proteins (Katayama, Harrison, and Toda, unpublished data). F-box proteins containing LRR (F/LRR) are ubiquitous among virtually all eukaryotes, and together with the F/WD type, comprise the most abundant form of this protein family (Cenciarelli *et al.*, 1999; Regan-Reiman *et al.*, 1999; Winston *et al.*, 1999). As mentioned previously, budding yeast, if not other eukaryotes, contain Fcl1, a protein structurally and functionally related to Pof3. Although at present proteins containing all three motifs, TPR/F/LRR, have not been identified in organisms other than yeast, given the ubiquitous presence of TPR and LRR motifs, we suspect that this type of F-box protein containing double modules might exist in other organisms.

On the other hand, it should be pointed out that despite the conservation of substrates of the SCF, there is a situation where F-box proteins have become diverged between yeast and vertebrates. For instance, cyclin-dependent kinase inhibitor in yeast, Rum1 in fission yeast, and Sic1 in budding yeast are degraded via Pop1/Pop2 and Cdc4, respectively, which are F/WD type (Patton *et al.*, 1998; Toda *et al.*, 1999), whereas in vertebrates it is Skp2, F/LRR type, which is responsible for SCF-mediated degradation of p27^{Kip1} (Nakayama *et al.*, 2001b). Thus, it is possible that functional, not structural homologs of Pof3/Fcl1, which play a role in genome integrity, exist in higher eukaryotes.

ACKNOWLEDGMENTS

We thank Drs. Robin Allshire, Tony Carr, Fumiko Esashi, Keith Gull, Fuyuki Ishikawa, Tomohiro Matsumoto, Hiroshi Murakami, Osami Niwa, Paul Nurse, Alison Pidoux, and Mitsuhiro Yanagida for strains and plasmids. We thank Drs. Jacqueline Hayles and Frank Uhlmann for critical reading of the manuscript, Mike Tyers and Mathias Peters for information on budding yeast Fcl1 before publication, Robin Allshire and Junko Kanoh for stimulating discussion, and Hiroshi Murakami and Satoko Yamaguchi for instructions in SDS-PAGE for the detection of phospho-Chk1. S.K. was supported by Japan Society for the Promotion of Science Postdoctoral Fellowships for Research Abroad. This work is supported by the Imperial Cancer Research Fund and the Human Frontier Science Program Research Grant.

REFERENCES

Adachi, Y., Toda, T., and Yanagida, M. (1986). Differential expression of essential and nonessential α-tubulin genes in *Schizosaccharomyces pombe*. Mol. Cell. Biol. *6*, 2168–2178.

Allshire, R.C., Nimmo, E.R., Ekwall, K., Javerzat, J.P., and Cranston, G. (1995). Mutations derepressing silent centromeric domains in fission yeast disrupt chromosome segregation. Genes Dev. *9*, 218–233.

Bähler, J., Wu, J., Longtine, M.S., Shah, N.G., McKenzie, A., III, Steever, A.B., Wach, A., Philippsen, P., and Pringle, J.R. (1998). Heterologous modules for efficient and versatile PCR-based gene targeting in *Schizosaccharomyces pombe*. Yeast *14*, 943–951.

Bai, C., Sen, P., Hofmann, K., Ma, L., Goebl, M., Harper, J.W., and Elledge, S.J. (1996). *SKP1* connects cell cycle regulators to the ubiquitin proteolysis machinery through a novel motif, the F-box. Cell *86*, 263–274.

Bannister, A.J., Zegerman, P., Partridge, J.F., Miska, E.A., Thomas, J.O., Allshire, R.C., and Kouzarides, T. (2001). Selective recognition of methylated lysine 9 on histone H3 by the HP1 chromo domain. Nature *410*, 120–124.

Basi, G., Schmid, E., and Maundrell, K. (1993). TATA box mutations in the *Schizosaccharomyces pombe nmt1* promoter affect transcriptional efficiency but not the transcription start point or thiamine repressibility. Gene *123*, 131–136.

Baumann, P., and Cech, T.R. (2000). Protection of telomeres by the Ku protein in fission yeast. Mol. Biol. Cell *11*, 3265–3275.

Baumann, P., and Cech, T.R. (2001). Pot1, the putative telomere end-binding protein in fission yeast and humans. Science *292*, 1171–1175.

Belenguer, P., Oustrin, M.-L., Tiraby, G., and Ducommun, B. (1995). Effects of phleomycin-induced DNA damage on the fission yeast *Schizosaccharomyces pombe*. Yeast *11*, 225–231.

Blondel, M., Galan, J.-M., Chi, Y., Lafourcade, C., Longaretti, C., Deshaies, R., and Peter, M. (2000). Nuclear-specific degradation of Far1 is controlled by the localization of the F-box protein Cdc4. EMBO J. *19*, 6085–6097.

Bridge, A.J., Morphew, M., Bartlett, R., and Hagan, I.M. (1998). The fission yeast SPB component Cut12 links bipolar spindle formation to mitotic control. Genes Dev. *12*, 927–942.

Carr, A.M., and Hoekstra, M.F. (1995). The cellular responses to DNA damage. Trends Cell Biol. *5*, 32–40.

Cenciarelli, C., Chiaur, D.S., Guardavaccaro, D., Parks, W., Vidal, M., and Pagano, M. (1999). Identification of a family of human F-box proteins. Curr. Biol. *9*, 1177–1179.

Chikashige, Y., Ding, D.-Q., Funabiki, H., Haraguchi, T., Mashiko, S., Yanagida, M., and Hiraoka, Y. (1994). Telomere-led premeiotic chromosome movement in fission yeast. Science *264*, 270–273.

Cimini, D., Howell, B., Maddox, P., Khodjakov, A., Degrassi, F., and Salmon, E.D. (2001). Merotelic kinetochore orientation is a major mechanism of aneuploidy in mitotic mammalian tissue cells. J. Cell Biol. *153*, 517–528.

Cooper, J.P. (2000). Telomere transitions in yeast: the end of the chromosome as we know it. Curr. Opin. Genet. Dev. *10*, 169–177.

Cooper, J.P., Nimmo, E.R., Allshire, R.C., and Cech, T.R. (1997). Regulation of telomere length and function by a Myb-domain protein in fission yeast. Nature *385*, 744–747.

Dahlén, M., Olsson, T., Kanter-Smoler, G., Ramne, A., and Sunnerhagen, P. (1998). Regulation of telomere length by checkpoint genes in *Schizosaccharomyces pombe*. Mol. Biol. Cell *9*, 611–621.

Ekwall, K., Javerzat, J.-P., Lorentz, A., Schmidt, H., Cranston, G., and Allshire, R. (1995). The chromodomain protein Swi6: a key component at fission yeast centromere. Science *269*, 1429–1431.

Ekwall, K., Nimmo, E.R., Javerzat, J.P., Borgstrom, B., Egel, R., Cranston, G., and Allshire, R. (1996). Mutations in the fission yeast silencing factors *clr4*$^+$ and *rik1*$^+$ disrupt the localization of the chromo domain protein Swi6p and impair centromere function. J. Cell Sci. *109*, 2637–2648.

Ekwall, K., and Partridge, J.F. (1999). Fission yeast chromosome analysis: fluorescence *in situ* hybridization (FISH) and chromatin immunoprecipitation (CHIP). In: Chromosome Structural Analysis, a Practical Approach, ed. W.A. Bickmore, Oxford, UK: Oxford University Press, 39–57.

Enoch, T., Carr, A.M., and Nurse, P. (1992). Fission yeast genes involved in coupling mitosis to completion of DNA replication. Genes Dev. *6*, 2035–2046.

Esashi, F., and Yanagida, M. (1999). Cdc2 phosphorylation of Crb2 is required for reestablishing cell cycle progression after the damage checkpoint. Mol. Cell *4*, 167–174.

Feldman, R.M.R., Correll, C.C., Kaplan, K.B., and Deshaies, R.J. (1997). A complex of Cdc4p, Skp1p, and Cdc53p/cullin catalyzes ubiquitination of the phosphorylated CDK inhibitor Sic1p. Cell *91*, 221–230.

Freeman-Cook, L.L., Sherman, J.M., Brachmann, C.B., Allshire, R.C., Boeke, J.D., and Pillus, L. (1999). The *Schizosaccharomyces pombe* *hst4*$^+$ gene is a *SIR2* homologue with silencing and centromeric functions. Mol. Biol. Cell *10*, 3171–3186.

Freemont, P.S. (2000). RING for destruction? Curr. Biol. *10*, R84–R87.

Furnari, B., Rhind, N., and Russell, P. (1997). Cdc25 mitotic inducer targeted by Chk1 DNA damage checkpoint kinase. Science *277*, 1495–1497.

Galan, J.M., Wiederkehr, A., Seol, J.H., Haguenauer-Tsapis, R., Deshaies, R.J., Riezman, H., and Peter, M. (2001). Skp1p and the F-box protein Rcy1p form a non-scf complex involved in recycling of the snare Snc1p in yeast. Mol. Cell. Biol. *21*, 3105–3117.

Goebl, M., and Yanagida, M. (1991). The TPR snap helix: a novel protein repeat motif from mitosis to transcription. Trends Biochem. Sci. *16*, 173–177.

Hartwell, L., Weinert, T., Kadyk, L., and Garvik, B. (1994). Cell cycle checkpoints, genomic integrity, and cancer. Cold Spring Harb. Symp. Quant. Biol. *59*, 259–263.

Hartwell, L.H., and Weinert, T.A. (1989). Checkpoints: controls that ensure the order of cell cycle events. Science *246*, 629–634.

Hershko, A., and Ciechanover, A. (1992). The ubiquitin system for protein degradation. Annu. Rev. Biochem. *61*, 761–807.

Hiraoka, Y., Henderson, E., and Blackburn, E.H. (1998). Not so peculiar: fission yeast telomere repeats. Trends Biochem. Sci. *23*, 126.

Hochstrasser, M. (1996). Ubiquitin-dependent protein degradation. Annu. Rev. Genet. *30*, 405–439.

Hoeijmakers, J.H. (2001). Genome maintenance mechanisms for preventing cancer. Nature *411*, 366–374.

Jackson, P.K., Eldridge, A.G., Freed, E., Furstenthal, L., Hsu, J.Y., Kaiser, B.K., and Reimann, J.D. (2000). The lore of the RINGs: substrate recognition and catalysis by ubiquitin ligases. Trends Cell Biol. *10*, 429–439.

Kaplan, K.B., Hyman, A.A., and Sorger, P.K. (1997). Regulating the yeast kinetochore by ubiquitin-dependent degradation and Skp1p-mediated phosphorylation. Cell *91*, 491–500.

Katayama, S., Hirata, D., Arellano, M., Pérez, P., and Toda, T. (1999). Fission yeast α-glucan synthase Mok1 requires the actin cytoskeleton to localize the sites of growth and plays an essential role in cell morphogenesis downstream of protein kinase C function. J. Cell Biol. *144*, 1173–1186.

Kim, S.H., Lin, D.P., Matsumoto, S., Kitazono, A., and Matsumoto, T. (1998). Fission yeast Slp1: an effector of the Mad2-dependent spindle checkpoint. Science *279*, 1045–1047.

Kobe, B., and Deisenhofer, J. (1994). The leucine-rich repeat: a versatile binding motif. Trends Biochem. Sci. *19*, 415–421.

Kominami, K., Ochotorena, I., and Toda, T. (1998). Two F-box/WD-repeat proteins Pop1 and Pop2 form hetero- and homo-complexes together with cullin-1 in the fission yeast SCF (Skp1-Cullin-1-F-box) ubiquitin ligase. Genes Cells *3*, 721–735.

Kominami, K., and Toda, T. (1997). Fission yeast WD-repeat protein Pop1 regulates genome ploidy through ubiquitin-proteasome-mediated degradation of the CDK inhibitor Rum1 and the S-phase initiator Cdc18. Genes Dev. *11*, 1548–1560.

Lengauer, C., Kinzler, K.W., and Vogelstein, B. (1998). Genetic instabilities in human cancers. Nature *396*, 643–649.

Lingner, J., and Cech, T.R. (1998). Telomerase and chromosome end maintenance. Curr. Opin. Genet. Dev. *8*, 226–232.

Manolis, K.G., Nimmo, E.R., Hartsuiker, E., Carr, A.M., Jeggo, P., A., and Allshire, R.C. (2001). Novel functional requirements for non-

homologous DNA end joining in *Schizosaccharomyces pombe*. EMBO J. *20*, 210–221.

Matsuura, A., Naito, T., and Ishikawa, F. (1999). Genetic control of telomere integrity in *Schizosaccharomyces pombe*: *rad3*$^+$ and *tel1*$^+$ are parts of two regulatory networks independent of the downstream protein kinases *chk1*$^+$ and *cds1*$^+$. Genetics *152*, 1501–1512.

McCready, S., Carr, A.M., and Lehmann, A.R. (1993). Repair of cyclobutane pyrimidine dimers and 6–4 photoproducts in the fission yeast *Schizosaccharomyces pombe*. Mol. Microbiol. *10*, 885–890.

Moreno, S., Klar, A., and Nurse, P. (1991). Molecular genetic analyses of fission yeast *Schizosaccharomyces pombe*. Methods Enzymol. *194*, 773–782.

Mori, T., Nakane, M., Hattori, T., Matsunaga, T., Ihara, M., and Nikaido, O. (1991). Simultaneous establishment of monoclonal antibodies specific for either cyclobutane pyrimidine dimer or (6-4) photoproduct from the same mouse immunized with ultraviolet-irradiated DNA. Photochem. Photobiol. *54*, 225–232.

Mundt, K.E., Porte, J., Murray, J.E., Brikos, C., Christensen, P.U., Caspari, T., Hagan, I.M., Millar, J.B.A., Simanis, V., Hofmann, K., and Carr, A.M. (1999). The COP9/signalosome complex is conserved in fission yeast and has a role in S phase. Curr. Biol. *9*, 1427–1430.

Murakami, H., and Nurse, P. (2000). DNA replication and damage checkpoints and the fission and budding yeasts. Biochem. J. *349*, 1–12.

Murakami, H., and Okayama, H. (1995). A kinase from fission yeast responsible for blocking mitosis in S phase. Nature *374*, 817–819.

Murray, A.W. (1995). The genetics of cell cycle checkpoints. Curr. Opin. Genet. *5*, 5–11.

Naito, T., Matsuura, A., and Ishikawa, F. (1998). Circular chromosome formation in a fission yeast mutant defective in two *ATM* homologues. Nature Genet. *20*, 203–206.

Nakamura, T.M., Morin, G.B., Chapman, K.B., Weinrich, S.L., Andrews, W.H., Lingner, J., Harley, C.B., and Cech, T.R. (1997). Telomerase catalytic subunit homologs from fission yeast and human. Science *277*, 955–959.

Nakayama, J., Rice, J.C., Strahl, B.D., Allis, C.D., and Grewal, S.I. (2001a). Role of histone H3 lysine 9 methylation in epigenetic control of heterochromatin assembly. Science *292*, 110–113.

Nakayama, K.I., Hatakeyama, S., and Nakayama, K. (2001b). Regulation of the cell cycle at the G_1-S transition by proteolysis of cyclin E and $p27^{Kip1}$. Biochem. Biophys. Res. Commun. *282*, 853–860.

Nasmyth, K., Peters, J.-M., and Uhlman, F. (2000). Splitting the chromosome: cutting the ties that bind sister chromatids. Science *288*, 1379–1384.

Nimmo, E.R., Cranston, G., and Allshire, R.C. (1994). Telomere-associated chromosome breakage in fission yeast results in variegated expression of adjacent genes. EMBO J. *13*, 3801–3811.

Niwa, O., Matsumoto, T., Chikashige, Y., and Yanagida, M. (1989). Characterization of *Schizosaccharomyces pombe* minichromosome deletion derivatives and a functional allocation of their centromere. EMBO J. *8*, 3045–3052.

Nurse, P. (1990). Universal control mechanism regulating onset of M-phase. Nature *344*, 503–508.

Olsson, T.G., Ekwall, K., Allshire, R.C., Sunnerhagen, P., Partridge, J.F., and Richardson, W.A. (1998). Genetic characterization of *hda1*$^+$, a putative fission yeast histone deacetylase gene. Nucleic Acids Res. *26*, 3247–3254.

Osaka, F., *et al*. (2000). Covalent modifier NEDD8 is essential for SCF ubiquitin-ligase in fission yeast. EMBO J. *19*, 3475–3484.

Patton, E.E., Willems, A.R., and Tyers, M. (1998). Combinatorial control in ubiquitin-dependent proteolysis: don't Skp the F-box hypothesis. Trends Genet. *14*, 236–243.

Peters, J.-M. (1998). SCF and APC: the Yin and Yang of cell cycle regulated proteolysis. Curr. Opin. Cell Biol. *10*, 759–768.

Pidoux, A.L., Uzawa, S., Perry, P.E., Cande, W.Z., and Allshire, R.C. (2000). Live analysis of lagging chromosomes during anaphase and their effect on spindle elongation rate in fission yeast. J. Cell Sci. *113*, 4177–4191.

Regan-Reiman, J.D., Duong, Q.V., and Jackson, P.K. (1999). Identification of novel F-box proteins in *Xenopus laevi*s. Curr. Biol. *9*, R762–R763.

Reimann, J.D.R., Freed, E., Hsu, J.Y., Kramer, E.H., Peters, J.-M., and Jackson, P.K. (2001). Emi1 is a mitotic regulator that interacts with Cdc2 and inhibits the anaphase promoting complex. Cell *105*, 645–655.

Rhind, N., and Russell, P. (2000). Chk1 and Cds1: linchpins of the DNA damage and replication checkpoint pathways. J. Cell Sci. *113*, 3889–3896.

Russell, P. (1998). Checkpoints on the road to mitosis. Trends Biol. Sci. *23*, 399–402.

Saka, Y., Esashi, F., Matsusaka, T., Mochida, S., and Yanagida, M. (1997). Damage and replication checkpoint control in fission yeast is ensured by interactions of Crb2, a protein with BRCT motif, with Cut5 and Chk1. Genes Dev. *11*, 3387–3400.

Seol, J.H., Shevchenko, A., Shevchenko, A., and Deshaies, R.J. (2001). Skp1 forms multiple protein complexes, including RAVE, a regulator of V-ATPase assembly. Nat. Cell Biol. *3*, 384–391.

Skowyra, D., Craig, K.L., Tyers, M., Elledge, S.J., and Harper, J.W. (1997). F-box proteins are receptors that recruit phosphorylated substrates to the SCF ubiquitin-ligase complex. Cell *91*, 209–219.

Steighner, R.J., and Povirk, L.F. (1990). Bleomycin-induced DNA lesions at mutational hot spots: implications for the mechanism of double-strand cleavage. Proc. Natl. Acad. Sci. USA *87*, 8350–8835.

Sugawara, N., and Szostak, J.W. (1986). Fission yeast telomere sequence. Yeast *2* (suppl), S373.

Toda, T., Ochotorena, I., and Kominami, K. (1999). Two distinct ubiquitin-proteolysis pathways in the fission yeast cell cycle. Phil. Trans. R. Soc. Lond. B Biol. Sci. *354*, 1551–1557.

Tyers, M., and Jorgensen, P. (2000). Proteolysis and the cell cycle: with this RING do thee destroy. Curr. Opin. Genet. Dev. *10*, 54–64.

Wang, S.-W., Norbury, C., Harris, A.L., and Toda, T. (1999). Caffeine can override the S-M checkpoint in fission yeast. J. Cell Sci. *112*, 927–937.

Willson, J., Wilson, S., Warr, N., and Watts, F.Z. (1997). Isolation and characterization of the *Schizosaccharomyces pombe rhp9* gene: a gene required for the DNA damage checkpoint but not the replication checkpoint. Nucleic Acids Res. *25*, 2138–2145.

Winston, J.T., Koepp, D.M., Zhu, C., Elledge, S.J., and Harper, J.W. (1999). A family of mammalian F-box proteins. Curr. Biol. *9*, 1180–1182.

Walworth, N.C., and Bernards, R. (1996). *rad*-dependent response of the *chk1*-encoded protein kinase at the DNA damage checkpoint. Science *271*, 353–356.

Yamano, H., Kitamura, K., Kominami, K., Lehmann, A., Katayama, S., Hunt, T., and Toda, T. (2000). The spike of S phase cyclin Cig2 expression at the G1-S border in fission yeast requires both APC and SCF ubiquitin ligases. Mol. Cell *6*, 1377–1387.

Zachariae, W., and Nasmyth, K. (1999). Whose end is destruction: cell division and the anaphase-promoting complex. Genes Dev. *13*, 2039–2058.